Article

Cell Reports

Conventional Dendritic Cells Confer Protection against Mouse Cytomegalovirus Infection via TLR9 and MyD88 Signaling

Graphical Abstract

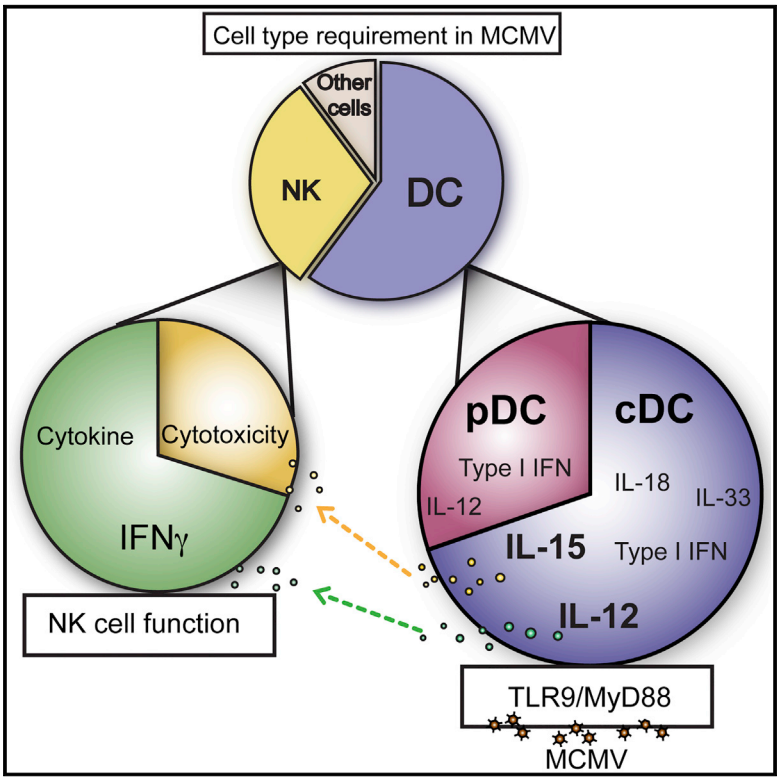

Highlights

- Generation of a mouse model to study DC-specific TLR9 function
- cDC uses TLR9- and MyD88-dependent mechanisms to promote MCMV immunity
- cDC-derived cytokines control independent NK cell effector responses against MCMV

Authors

Franz Puttur, Marcela Francozo, Gülhas Solmaz, ..., Hermann Wagner, Luciana Berod, Tim Sparwasser

Correspondence

tim.sparwasser@twincore.de

In Brief

Puttur et al. generate TLR9 conditional knockout mice to understand how individual DC subsets mechanistically regulate NK cell immunity during MCMV infection. By genetically deleting TLR9 or reactivating MyD88 function in DC subsets, they demonstrate that TLR9/MyD88 signaling in cDCs choreographs early MCMV immunity, providing targets for future therapies.

Puttur et al., 2016, Cell Reports *17*, 1113–1127
October 18, 2016
http://dx.doi.org/10.1016/j.celrep.2016.09.055

Cell Reports
Article

OPEN ACCESS
CellPress

Conventional Dendritic Cells Confer Protection against Mouse Cytomegalovirus Infection via TLR9 and MyD88 Signaling

Franz Puttur,[1,11] Marcela Francozo,[1,2,11] Gülhas Solmaz,[1] Carlos Bueno,[1,3] Marc Lindenberg,[1] Melanie Gohmert,[1] Maxine Swallow,[1] Dejene Tufa,[4] Roland Jacobs,[4] Stefan Lienenklaus,[5,6] Anja A. Kühl,[7] Lisa Borkner,[8] Luka Cicin-Sain,[8] Bernard Holzmann,[9] Hermann Wagner,[10] Luciana Berod,[1] and Tim Sparwasser[1,12,*]

[1]Institute of Infection Immunology, Centre for Experimental and Clinical Infection Research (Twincore), Hannover Medical School (MHH) and Helmholtz Centre for Infection Research (HZI), 30625 Hannover, Germany
[2]Ribeirão Preto Medical School, University of São Paulo, Avenida Bandeirantes 3900, Ribeirão Preto, São Paulo 14049-900, Brazil
[3]Laboratorio de Virología, Departamento de Química Biológica, IQUIBICEN, Facultad de Ciencias Exactas y Naturales, Universidad de Buenos Aires, Ciudad Universitaria, Buenos Aires C1428EGA, Argentina
[4]Department of Clinical Immunology and Rheumatology, MHH, 30625 Hannover, Germany
[5]Institute for Laboratory Animal Science, MHH, Carl-Neuberg-Strasse 1, 30625 Hannover, Germany
[6]Institute for Experimental Infection Research, Twincore, MHH and HZI, Feodor-Lynen-Strasse 7, 30625 Hannover, Germany
[7]Medical Department (Gastroenterology, Infectious Diseases and Rheumatology)/Research Center ImmunoScience, Charité–Universitätsmedizin Berlin, Campus Benjamin Franklin, 12200 Berlin, Germany
[8]Department for Vaccinology/Immune Aging and Chronic Infection, HZI, 38124 Braunschweig, Germany
[9]Department of Surgery, Technische Universität München, 81675 Munich, Germany
[10]Institute for Medical Microbiology, Immunology and Hygiene, Technische Universität München, 81675 Munich, Germany
[11]Co-first author
[12]Lead Contact
*Correspondence: tim.sparwasser@twincore.de
http://dx.doi.org/10.1016/j.celrep.2016.09.055

SUMMARY

Cytomegalovirus (CMV) is an opportunistic virus severely infecting immunocompromised individuals. In mice, endosomal Toll-like receptor 9 (TLR9) and downstream myeloid differentiation factor 88 (MyD88) are central to activating innate immune responses against mouse CMV (MCMV). In this respect, the cell-specific contribution of these pathways in initiating anti-MCMV immunity remains unclear. Using transgenic mice, we demonstrate that TLR9/MyD88 signaling selectively in CD11c$^+$ dendritic cells (DCs) strongly enhances MCMV clearance by boosting natural killer (NK) cell CD69 expression and IFN-γ production. In addition, we show that in the absence of plasmacytoid DCs (pDCs), conventional DCs (cDCs) promote robust NK cell effector function and MCMV clearance in a TLR9/MyD88-dependent manner. Simultaneously, cDC-derived IL-15 regulates NK cell degranulation by TLR9/MyD88-independent mechanisms. Overall, we compartmentalize the cellular contribution of TLR9 and MyD88 signaling in individual DC subsets and evaluate the mechanism by which cDCs control MCMV immunity.

INTRODUCTION

Cytomegalovirus (CMV) exhibits a broad tropism in humans, leading to a diverse range of infection-associated pathologies (Tabeta et al., 2004). In immunocompromised people, such as AIDS and transplant patients, as well as in unborn individuals infected during gestation, CMV is highly pathogenic. Despite numerous efforts, no effective vaccine exists against CMV (Ahmed, 2011). Furthermore, current anti-viral therapy is associated with numerous drawbacks, such as poor bioavailability, development of anti-viral drug resistance, and associated cytotoxicities (Plotkin, 2015). This warrants for an urgent requirement to design alternative approaches to enhance immune responses against CMV.

Mouse CMV (MCMV) is a natural pathogen in mice. The MCMV model of infection recapitulates the key immunological hallmarks of human CMV (HCMV) infection and is broadly used as a tool for studying immune responses against CMV. MCMV exhibits a broad cellular tropism (Krmpotic et al., 2003) with defined kinetics. After systemic infection, the spleen serves as an initial reservoir for MCMV replication, promoting the dissemination of virus to other organs (Alexandre et al., 2014). Viral replication commences in non-hematopoietic stromal cells 6–8 hr post-infection (p.i.), and virus disseminates to splenic red pulp cells by 17 hr before reaching the white pulp cells between day 1.5 and day 2 p.i. (Hsu et al., 2009), when conventional dendritic cells (cDCs) and plasmacytoid dendritic cells (pDCs) produce cytokines including type I interferon (IFN-I) and interleukin (IL) 12 (Dalod et al., 2002; Zucchini et al., 2008a). Dendritic cell (DC)-derived cytokines promote host survival by facilitating natural killer (NK) cell proliferation and effector function (Dalod et al., 2003; Nguyen et al., 2002) and blocking viral replication (Orange and Biron, 1996a). Specifically, IL-12 has been shown to induce NK cell-mediated interferon (IFN)-γ production, while IFN-I promotes IL-15-induced NK cell survival and cytotoxic

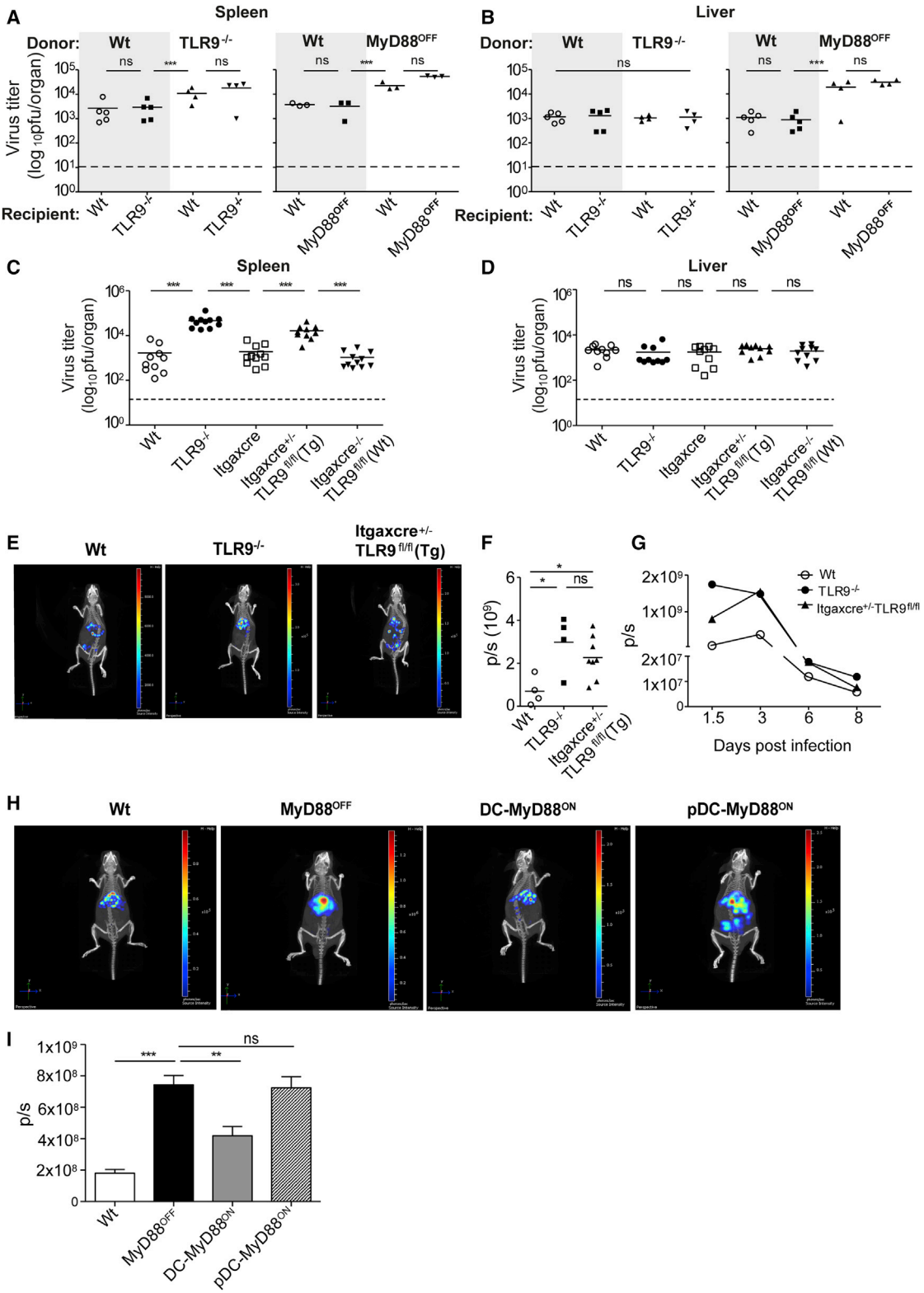

Figure 1. TLR9 and MyD88 Signaling in CD11c$^+$ Cells Controls MCMV Infection In Vivo

(A and B) Lethally irradiated recipient CD45.1 WT mice were reconstituted with donor CD45.2 WT, TLR9$^{-/-}$, or MyD88^{OFF} BM or irradiated recipient CD45.2 WT, TLR9$^{-/-}$, or MyD88^{OFF} mice were reconstituted with WT BM and then infected i.p. with 5 × 10^5 PFUs of MCMV. Viral load in the spleen (A) and in the liver (B) were evaluated at day 1.5 p.i.

(legend continued on next page)

capacity (Baranek et al., 2012; Nguyen et al., 2002; Orange and Biron, 1996a, 1996b). Simultaneously, MCMV-induced IL-18 enhances secretion of IFN-γ by NK cells (Pien et al., 2000), as well as Ly49H$^+$ NK cell expansion in the spleen (Andrews et al., 2003); however, it is not critical for NK cell-mediated protection against MCMV (Cocita et al., 2015), because IL-18$^{-/-}$ mice survive the infection (Pien et al., 2000). Despite the important role of pDC-derived cytokines, ablation of pDCs by anti-PDCA-1/Bst2/120G8 antibody (Cocita et al., 2015) or by diphtheria toxin (DT) injection in blood dendritic cell antigen 2 (BDCA2)-diphtheria toxin receptor (DTR) transgenic mice (Swiecki et al., 2010) minimally influences NK cell activation. These findings suggest that NK cell function during MCMV infection is not governed solely by signals derived from pDCs but may also depend on immunological cues from other cell types.

Pro-inflammatory cytokine production is triggered by direct sensing of MCMV, which occurs primarily through endosomal Toll-like receptor (TLR) 9, along with a partial redundancy for TLR7 (Zucchini et al., 2008b). Both TLR9 and TLR7 signal via the downstream adaptor molecule myeloid differentiation factor 88 (MyD88) (Delale et al., 2005; Krug et al., 2004; Tabeta et al., 2004). Complete loss of TLR9 or MyD88 in mice severely compromises MCMV clearance from infected organs (Krug et al., 2004; Zucchini et al., 2008b). This impaired resistance to MCMV in TLR9 and MyD88 knockout (KO) (−/−) mice is primarily attributed to reduced IFN-I production and NK cell activation (Krug et al., 2004; Zucchini et al., 2008b). The induction of IFN-I after systemic MCMV infection has been shown to be biphasic (Schneider et al., 2008). The first short-lived peak at 8 hr p.i. is mainly stromal cell derived, while the second, more sustained peak from day 1.5 p.i. (Schneider et al., 2008) is pDC derived (Dalod et al., 2002). It remains unclear whether stromal cells, in addition to DCs, contribute to protection against MCMV at the early phase of infection. In this regard, the cell-specific requirement of TLR9 and MyD88 signaling in the immune control of MCMV infection warrants a rigorous investigation.

To address these questions, we generated bone marrow (BM) chimeric mice lacking TLR9 or MyD88 in hematopoietic cells or non-hematopoietic cells, as well as transgenic mice with selective deletion of TLR9 or reactivation of MyD88 in CD11c$^+$ cells. In addition, using a mouse model in which CD11c$^+$ cells can be selectively depleted by administration of DT, we compare the contribution of TLR9 and MyD88 sensing by cDCs versus pDCs in controlling MCMV. By generating genetically engineered mice to target DC subsets in vivo after MCMV infection, we show that the loss of pDC-derived signals can be compensated by TLR9 and MyD88 signaling in cDCs, promoting NK cell activation, cytokine production, and viral clearance. Overall, we demonstrate a previously less understood function of cDCs in shaping immune responses to MCMV by using TLR9/MyD88-dependent mechanisms.

RESULTS

TLR9 and MyD88 Function in CD11c$^+$ Cells Controls MCMV Clearance

To carefully compartmentalize the contribution of TLR9 and MyD88 signaling in hematopoietic versus non-hematopoietic cells during MCMV infection, we generated wild-type (WT), TLR9$^{-/-}$, and MyD88^{OFF} (harboring a floxed transcriptional termination element between exons 1 and 2 of the *Myd88* gene) (Gais et al., 2012) BM chimeric mice. These mice lack either TLR9 or MyD88 in hematopoietic, non-hematopoietic, or both compartments. Chimeric mice were infected with MCMV, and spleen and liver were harvested at day 1.5 p.i. to determine the viral load. Mice lacking TLR9 or MyD88 only in the hematopoietic compartment exhibited significantly higher viral load in the spleen than WT chimeric mice (Figure 1A). In contrast, viral load in the liver was MyD88 dependent but TLR9 independent (Figure 1B). In addition, mice that lack TLR9 or MyD88 in non-hematopoietic cells alone have comparable viral titers to WT chimeric mice (Figures 1A and 1B), excluding a contribution of the TLR9/MyD88 pathways in this compartment. Altogether, our data clearly indicate that TLR9/MyD88 signaling in hematopoietic cells is sufficient to control MCMV in the spleen at day 1.5 p.i.

Next, we addressed the cell-specific role of TLR9 in DCs and its consequent impact on MCMV clearance by generating useful genetically engineered loxP-flanked TLR9 (TLR9 flox, or TLR9$^{fl/fl}$) mice (Figure S1A), in which exon 2 (carrying the main coding sequence) of the *Tlr9* gene is flanked by loxP sites. TLR9$^{fl/fl}$ mice were crossed to CD11c Cre mice (expressing Cre recombinase under the control of the Itgax promoter) (Caton et al., 2007), thereby allowing selective deletion of TLR9 in CD11c$^+$ cells. These mice are further denoted as ItgaxCre$^{+/-}$TLR9$^{fl/fl}$. Cre expression in ItgaxCre mice was demonstrated to occur predominantly in DCs (95% of CD11c^{high} cDCs and 50%–80% of pDCs), with a low amount of recombination in T lymphocytes (<10%), NK cells (12%), and myeloid cells (<1%) (Caton et al., 2007). Similarly, in our conditional KO mice, in which Cre expression is driven by the same CD11c promoter, TLR9 is efficiently deleted in both cDC and pDC subsets (Figure S1B), resulting in the loss of DC-specific TLR9 function upon stimulation (Figures S1C and S1D). Infection of these mice with MCMV indicates that by day 1.5 p.i., the viral load in the spleen was comparable to that in TLR9$^{-/-}$ mice and significantly higher than that in WT controls (Figure 1C), whereas titers in the liver were similar in all groups (Figure 1D). This finding is in concordance with the results displayed in Figure 1B, demonstrating that the anti-viral

(C and D) WT (C57BL/6), TLR9$^{-/-}$, ItgaxCre, and ItgaxCre$^{+/-}$TLR9$^{fl/fl}$ and littermate controls ItgaxCre$^{-/-}$TLR9$^{fl/fl}$ were infected with 5 × 10^5 PFUs MCMV. Viral load was determined in the spleen (C) and liver (D) at day 1.5 p.i. (C) and (D) are pooled data from three experiments with n = 3–4 mice per group.
(E–I) WT, TLR9$^{-/-}$, DC-MyD88^{ON}, pDC-MyD88^{ON}, and MyD88^{OFF} were infected i.p. with MCMV luciferase at 5 × 10^5 PFUs. (E and H) Intravital imaging displaying an overlay of viral bioluminescence, with mouse computer tomography scan showing MCMV viral load in the abdominal cavity at day 1.5 p.i. of WT, TLR9$^{-/-}$, and ItgaxCre$^{+/-}$TLR9$^{fl/fl}$ mice (E) and WT, MyD88^{OFF}, DC-MyD88^{ON}, and pDC-MyD88^{ON} mice (H). Photon flux (p/s) quantification is shown at day 1.5 p.i. (F, G, and I) and days 3, 6, and 8 p.i. (G). Data are from one of three individual experiments with similar results. n = 3–4 mice/group/experiment.
NS, not significant; ***p < 0.001, **p < 0.01, *p < 0.05; Kruskal-Wallis test.

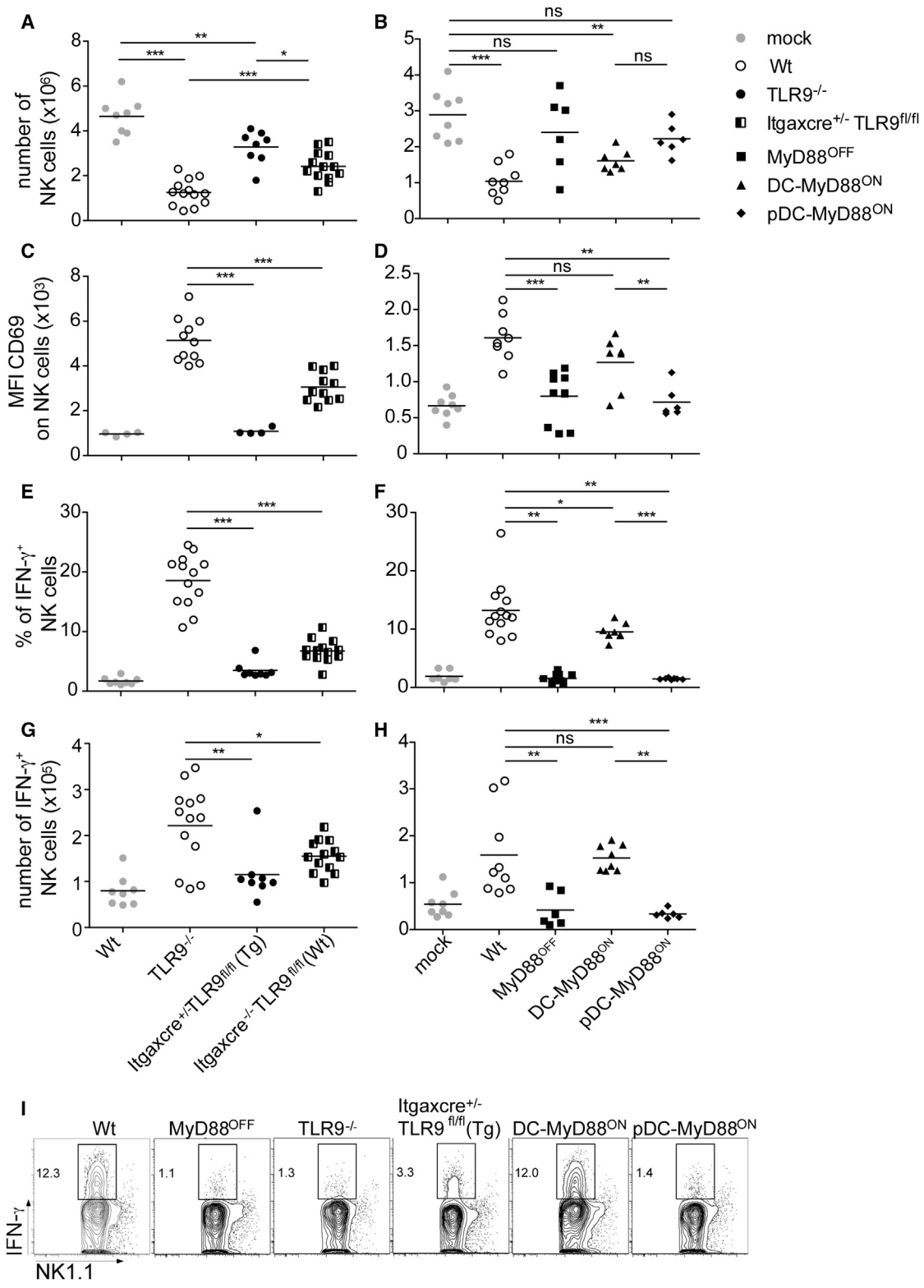

Figure 2. NK Cell Activation and Function Are Compromised in Mice Lacking TLR9 and MyD88 Signaling in CD11c$^+$ Cells

(A–H) TLR9$^{-/-}$, ItgaxCre$^{+/-}$TLR9$^{fl/fl}$, and ItgaxCre$^{-/-}$TLR9$^{fl/fl}$ mice (A, C, E, and G) and WT, MyD88^{OFF}, DC-MyD88^{ON}, and pDC-MyD88^{ON} mice (B, D, F, and H) were infected with 5 × 10^5 PFUs of MCMV or PBS treated (Mock), and spleens were harvested at day 1.5 p.i. (A and B) Total number of NK cells (NK1.1$^+$CD3$^-$).

(legend continued on next page)

response in the liver at day 1.5 p.i. is TLR9 independent. In contrast, the viral load in LysMCre$^{+/-}$TLR9$^{fl/fl}$ mice, in which TLR9 deletion occurs in LysM^{+} cells (Clausen et al., 1999) such as macrophages and neutrophils, was comparable to that in WT mice (Figures S2A and S2B). We then examined MCMV load at day 1.5 p.i. using a luciferase-expressing strain of MCMV and intravital imaging. The strength of the bioluminescent signal, which correlates to viral burden, was significantly higher in the peritoneum of mice lacking TLR9 (TLR9$^{-/-}$) or Itgax-Cre$^{+/-}$TLR9$^{fl/fl}$ mice than in WT controls (Figures 1E and 1F). The overall bioluminescent signal between TLR9$^{-/-}$ and Itgax-Cre$^{+/-}$TLR9$^{fl/fl}$ mice was comparable with minor variation in virus distribution across the peritoneum (Figure S2C). Furthermore, luminescence remained high until day 3 p.i. and decreased by day 8 p.i., when infection was cleared in all mice (Figure 1G).

To investigate the importance of MyD88 in DCs, we next crossed ItgaxCre mice (Caton et al., 2007) or pDCre mice (Puttur et al., 2013) with MyD88^{OFF} mice. The mice generated from these crossings, here termed DC-MyD88^{ON} and pDC-MyD88^{ON}, reactivate *Myd88* gene expression in CD11c^{+} cells or in Siglec-H^{+} cells, respectively, and have been carefully characterized in our previous work (Arnold-Schrauf et al., 2014; Berod et al., 2014; Dudek et al., 2016). Reactivation of MyD88 in CD11c^{+} cells (DC-MyD88^{ON}) significantly improved clearance of MCMV compared to mice that reactivated MyD88 only in a representative fraction of pDCs (pDC-MyD88^{ON}) or mice that lacked MyD88 in all cells (MyD88^{OFF}) (Figures 1H and 1I). Overall, our findings suggest that TLR9 and MyD88 signaling in CD11c^{+} cells is mandatory to control splenic MCMV infection at day 1.5 p.i.

NK Cell Activation and IFN-γ Production Are Compromised in Mice Lacking TLR9 and MyD88 Signaling in CD11c^{+} Cells

NK cells are central players in promoting host immune responses against MCMV by rapidly secreting cytokines and releasing cytotoxic granules to kill infected cells (Lodoen and Lanier, 2006). MCMV is sensed predominantly by TLR9, and mice deficient in TLR9 show significantly reduced NK cell CD69 expression and NK cell IFN-γ production after 2 days of infection (Krug et al., 2004). Given that ItgaxCre$^{+/-}$TLR9$^{fl/fl}$ mice and DC-MyD88^{ON} mice showed complementary effects in MCMV clearance, we next evaluated NK cell responses in these mice. NK T cells were excluded by co-staining with anti-CD3 antibody (Figure S3). Following systemic MCMV infection, splenic NK cells rapidly undergo cytokine-driven proliferation and contraction due to cellular apoptosis (Dokun et al., 2001; Robbins et al., 2004; Schlub et al., 2011; Stacey et al., 2011). Similarly, in our infection model, WT mice showed a significant reduction in the total number of NK cells present in the spleen at day 1.5 p.i. compared to the mock-infected controls (Figures 2A and 2B). This contraction in the number of NK cells was less pronounced in TLR9$^{-/-}$, ItgaxCre$^{+/-}$TLR9$^{fl/fl}$, and MyD88^{OFF} mice (Figures 2A and 2B). In addition, during the early phase of infection, reactivation of MyD88 in CD11c^{+} cells led to a similar reduction in the number of NK cells compared to WT mice, whereas pDC-MyD88^{ON} mice failed to induce NK cell contraction (Figure 2B). Besides, complete or CD11c-specific deletion of TLR9/MyD88 signaling strongly reduced the mean fluorescence intensity (MFI) of CD69 on NK cells (Figures 2C and 2D) and the frequency and number of IFN-γ^{+} NK cells (Figures 2E, 2G, and 2I). Complementary effects were observed when MyD88 was reactivated in CD11c^{+} cells, increasing expression of CD69 on NK cells (Figure 2D), as well as the frequency (Figures 2F and 2I) and number (Figure 2H) of IFN-γ^{+} NK cells. Reactivation of MyD88 in pDCs was not sufficient to restore CD69 expression and IFN-γ to WT levels. Our results show that NK cell activation and IFN-γ production are regulated by TLR9/MyD88-derived signals from CD11c^{+} cells, which are mainly DCs.

After the initial contraction phase, NK cells proliferate and expand between day 2 and day 7 p.i. (Schlub et al., 2011). This NK cell expansion is mostly restricted to Ly49H^{+} NK cells recognizing m157 (Min-Oo and Lanier, 2014) and is phenotypically characterized by KLRG1 expression (Robbins et al., 2004). We evaluated the frequencies of KLRG1^{+}Ly49H^{+} versus KLRG1^{+} Ly49H^{-} NK cells at day 8 p.i. and observed that infection increased the frequencies of KLRG1^{+} expressing Ly49H^{+} NK cells to a similar extent in WT and ItgaxCre$^{+/-}$TLR9$^{fl/fl}$ mice compared to mock mice (Figure S4). This suggests that TLR9 function in CD11c^{+} cells may only influence the early NK cell response.

NK Cell Cytotoxicity Is Independent of TLR9 and MyD88 Function

Because CD11c-driven TLR9 and MyD88 signaling strongly contributed to NK cell CD69 expression and IFN-γ production, we next evaluated the cytotoxic capacity of NK cells. Surprisingly, compared to WT, the ability of NK cells to kill YAC-1 target cells at day 1.5 p.i. remained unchanged in the absence of TLR9 or MyD88 (Figure 3A). NK cell cytotoxicity has been shown to be promoted by IFN-I (Andoniou et al., 2005; Nguyen et al., 2002). However, although a role for IFN-α in NK cell cytotoxic activity during MCMV infection was previously ruled out (Orange and Biron, 1996b), the contribution of IFN-β remains unclear. For example, in IRF7$^{-/-}$ mice that lack IFN-α, normal NK cell degranulation has been related to the presence of IFN-β (Steinberg et al., 2009). To test this hypothesis, IRF7$^{-/-}$ mice (Honda et al., 2005) were bred to an IFN-β reporter mouse (Lienenklaus et al., 2009) (referred to as IFN-β$^{WT/\Delta}$ in our study). Mice bred heterozygously for the targeted Δβluc mutation (IRF7$^{-/-}$IFN-β$^{WT/\Delta}$) have normal IFN-β production due to the presence of a functional WT allele, whereas homozygous (IRF7$^{-/-}$IFN-β$^{\Delta/\Delta}$) mice lack IFN-β after systemic MCMV infection (Figure S5). MCMV-infected IRF7$^{-/-}$ mice show comparable levels of NK cell cytotoxicity (Figure 3B) and NK cell degranulation, as evidenced by

(C and D) MFI of CD69 expression on splenic NK cells. (E–H) Splenocytes were incubated with IL-2 (2 hr) and brefeldin A (4 hr). Frequencies (E and F) and numbers (G and H) of IFN-γ^{+} NK cells are depicted for the individual mice.

(I) Representative flow cytometry plots of graphs shown in (E) and (F).

Data are pooled from one of two individual experiments with similar results. n = 3–5 mice/group; NS, not significant; ***p < 0.001, **p < 0.01, *p < 0.05; one-way ANOVA with Tukey post test.

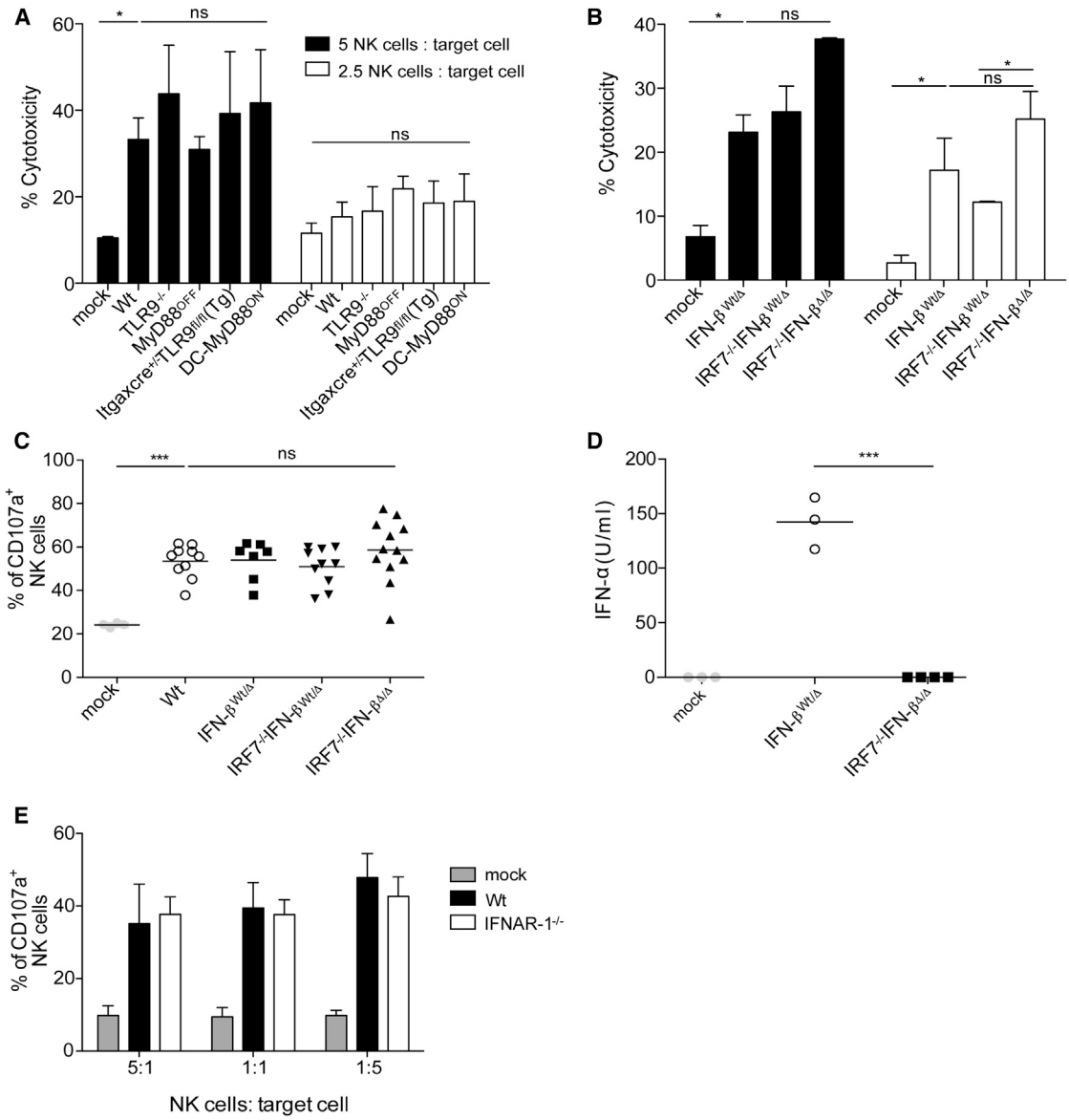

Figure 3. NK Cell Cytotoxicity Is Independent of TLR9 and MyD88 Signaling

(A) TLR9$^{-/-}$, ItgaxCre$^{+/-}$TLR9$^{fl/fl}$, ItgaxCre$^{-/-}$TLR9$^{fl/fl}$, MyD88^{OFF}, DC-MyD88^{ON}, and pDC-MyD88^{ON} mice were infected with 5 × 10^5 PFUs of MCMV. Spleens were harvested at day 1.5 p.i., and NK cells were sorted for chromium release assays.

(B and C) To exclude the contribution of IFN-β in NK cell cytotoxicity, splenic NK cells were sorted from IRF7$^{-/-}$IFN-β$^{Δ/Δ}$ mice for chromium release assays (B) and CD107a degranulation assays (C).

(D) IFN-α levels at day 1.5 p.i. in sera of IRF7$^{-/-}$IFN-β$^{Δ/Δ}$ mice compared to infected control IFN-β$^{WT/Δ}$ mice.

(E) NK cell degranulation in WT control and IFNAR-1$^{-/-}$ mice.

Data are from one of two individual experiments with similar results. n = 3–5 mice/group ± SD; NS, not significant; ***p < 0.001, **p < 0.01, *p < 0.05; one-way ANOVA with Tukey post test.

CD107a expression (Figure 3C), like IRF7$^{-/-}$IFN-β$^{WT/Δ}$ or IFN-β$^{WT/Δ}$ mice. No IFN-α can be detected in the serum of IRF7$^{-/-}$IFN-β$^{Δ/Δ}$ mice, excluding a contribution of residual IFN-α to NK cell-mediated cytotoxicity (Figure 3D). Finally, we ruled out the involvement of IFN-I in NK cell degranulation by using IFNAR-1$^{-/-}$ mice, because we observed comparable NK cell degranulation between MCMV-infected IFNAR-1$^{-/-}$ and WT mice (Figure 3E). Overall, our results show that NK cell degranulation and cytotoxic capacity upon MCMV infection are TLR9/MyD88 and IFN-I independent.

TLR9/MyD88 Signaling in CD11c$^+$ Cells Regulates the Anti-viral Cytokine Response to MCMV

Pro-inflammatory DC-derived cytokines, specifically IFN-I and IL-12, promote NK cell activation and cytokine production after MCMV infection (Baranek et al., 2012; Orange and Biron,

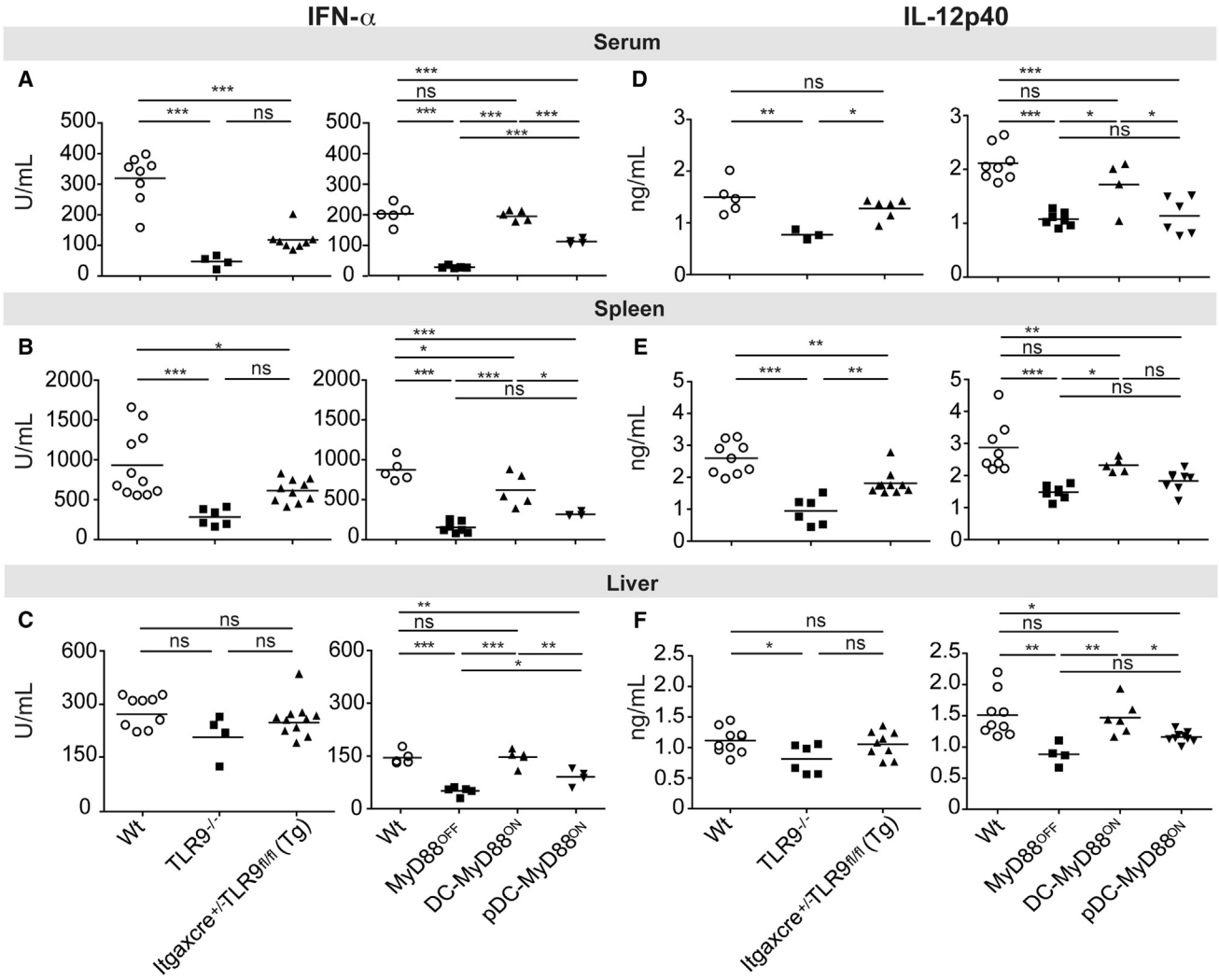

Figure 4. TLR9/MyD88 in DCs Regulates the Pro-inflammatory Cytokine Response against MCMV

(A–F) WT, TLR9$^{-/-}$, ItgaxCre$^{+/-}$TLR9$^{fl/fl}$, MyD88^{OFF}, DC-MyD88^{ON}, and pDC-MyD88^{ON} mice were infected with 5 × 10^5 PFUs of MCMV. IFN-α (A–C) and IL-12p40 (D–F) levels were measured in serum (A and D) and lysates of spleen (B and E) and liver (C and F) on day 1.5 p.i.

Data are from one of two individual experiments with similar results. n = 3–5 mice/group ± SD; NS, not significant; ***p < 0.001, **p < 0.01, *p < 0.05; one-way ANOVA with Tukey post test.

1996b). Splenic pDCs are the major producers of IFN-I at day 1.5 p.i. (Asselin-Paturel et al., 2001; Dalod et al., 2002; Krug et al., 2004; Scheu et al., 2008; Zucchini et al., 2008a), while IL-12 can be produced by various DC subsets (Alexandre et al., 2014; Dalod et al., 2002). To better define the contribution of cDCs and pDCs for NK cell activation, we next evaluated IL-12p40 and IFN-α concentrations upon infection. Complete or CD11c-specific deletion of TLR9/MyD88 signaling leads to significantly reduced IFN-α levels in the serum and spleen (Figures 4A and 4B) compared to infected controls, whereas IL-12p40 production is modestly reduced (Figures 4D and 4E). Consistent with the viral load (Figure 1), production of proinflammatory cytokines in the liver is MyD88 dependent but TLR9 independent (Figures 4C and 4F). In turn, reactivation of MyD88 in CD11c$^+$ cells strongly restores IFN-α and IL-12p40 production in the serum (Figures 4A and 4D), spleen (Figures 4B and 4E), and liver (Figures 4C and 4F). IFN-α levels, but not IL-12p40 levels, also increased significantly in the serum and liver of pDC-MyD88^{ON} mice compared to MyD88^{OFF} mice; however, the increase was not as pronounced as that observed in DC-MyD88^{ON} mice, in which MyD88 is reactivated in both cDCs and pDCs (Figures 4A–4F) and is likely more efficiently in pDCs from DC-MyD88ON mice than is the case for pDC-MyD88^{ON} mice.

NK Cell Effector Function Is Primarily Regulated by DC-Derived Cytokines in a TLR9/MyD88-Dependent Manner

NK cells have been shown to directly sense MCMV-infected cells via MyD88 (Cocita et al., 2015). In DC-MyD88^{ON} mice, we observe an intermediate reactivation of MyD88 in NK cells (Figure S6). Hence, to rule out the direct activation of NK cells by

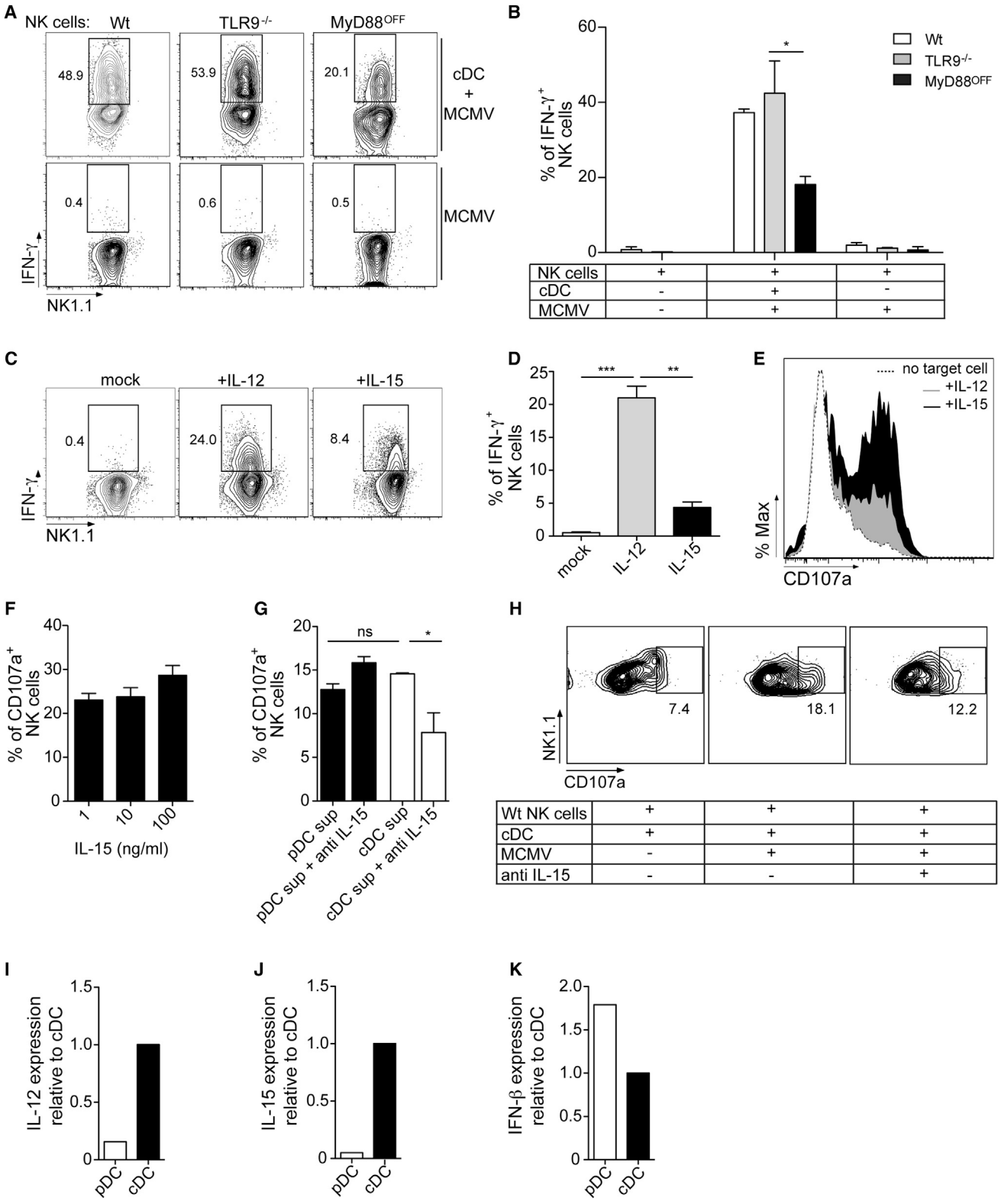

Figure 5. NK Cell Effector Function Is Primarily Regulated by DC-Derived Cytokines in a TLR9/MyD88-Dependent Manner

Sorted NK cells from WT, TLR9$^{-/-}$, and MyD88^{OFF} mice were cultured in vitro with or without DCs and infected with MCMV (MOI 2) for 24 hrs. (A and B) Intracellular IFN-γ expression in NK cells is shown in (A) as representative flow cytometric plots and in (B) as the frequency of IFN-γ^{+} NK cells.

(legend continued on next page)

MCMV in our experimental setting, we co-cultured WT, TLR9$^{-/-}$, and MyD88^{OFF} NK cells with MCMV alone or with cDCs and determined NK cell IFN-γ production. In the absence of cDCs, NK cells in all groups fail to produce IFN-γ by direct sensing of MCMV (Figure 5A). However, addition of WT cDCs to the culture significantly enhanced IFN-γ production in WT and TLR9$^{-/-}$ and to a lesser extent in MyD88^{OFF} NK cells (Figures 5A and 5B). The latter can be explained by previous reports showing that during MCMV infection, the cytokines IL-18 and IL-33 activate NK cells via MyD88 (Madera and Sun, 2015; Nabekura et al., 2015). Likewise, MyD88-deficient NK cells were demonstrated to have a reduced ability to induce IFN-γ production, whereas no effect on NK cell degranulation was observed (Cocita et al., 2015; Madera and Sun, 2015; Nabekura et al., 2015).

Supporting the importance of DC-derived cytokines, the addition of exogenous IL-12 boosts NK cell IFN-γ production while IL-15 shows only a minor effect (Figures 5C and 5D). The reverse is seen for NK cell degranulation, in which IL-15 is significantly more potent than IL-12 (Figure 5E). This IL-15-mediated effect is dose dependent (Figure 5F). To further evaluate the contribution of cDC- versus pDC-derived IL-15 to NK cell degranulation, we sorted fms-like tyrosine kinase 3 ligand (Flt3-L)-differentiated pDCs and cDCs and infected them with MCMV for 24 hrs in vitro. NK cells were then cultured in the presence of conditioned supernatant from infected cDCs or pDCs with or without neutralizing antibody against IL-15. Both cDC and pDC supernatants increased the percentage of CD107a^{+} NK cells to a similar extent, but IL-15 neutralization prevented only cDC-mediated NK cell degranulation (Figure 5G). Consistently, addition of anti-IL-15 to MCMV-infected cDC-NK cell co-cultures dampened NK cell degranulation (Figure 5H). To examine whether in vivo IL-15 was also cDC derived, we infected WT mice with MCMV for 1.5 days and sorted splenic pDCs and cDCs for RT-PCR analysis. Our results confirm that upon in vivo infection, cDCs are the predominant source of IL-12p40 and IL-15, while IFN-β is primarily produced by pDCs (Figures 5I–5K) in accordance with earlier studies (Nguyen et al., 2002; Zucchini et al., 2008a). Altogether, our results show that CD11c^{+} DCs are required for cytokine-driven activation of NK cells and cDC-derived IL-12p40 and IL-15 regulate independent arms of NK cell function during MCMV infection.

TLR9 and MyD88 Signaling in cDCs Promotes Robust NK Cell Activation and Efficient Viral Clearance

In ItgaxCre$^{+/-}$TLR9$^{fl/fl}$ and DC-MyD88^{ON} mice, both cDCs and pDCs are targeted (Caton et al., 2007). Hence, our results obtained thus far provide a holistic view on the TLR9/MyD88 signaling events derived from both DC subsets. To study the relevance of TLR9 and MyD88 signaling in individual DC subsets during MCMV infection, we adopted the ItgaxCre-iDTR (induced diphtheria toxin receptor) mouse model, in which CD11c^{+} cells can be depleted by administering DT (Buch et al., 2005). Because pDCs express intermediate levels of CD11c (Arnold-Schrauf et al., 2015), we first checked the depletion efficiency of both DC subsets in vivo. Before infection, one round of DT efficiently depleted cDCs and pDCs (Figure S7A). Furthermore, given that NK cells can also express CD11c, ItgaxCre mice were crossed to floxed red fluorescent protein (RFP) reporter mice (termed ItgaxCre$^{+/-}$ RFP^{+}) (Luche et al., 2007), thereby terminally labeling all CD11c^{+} cells. Immunostainings of spleen sections and flow cytometry analysis confirmed a minor fraction of RFP^{+} NK cells (Figure S7B). However, DT treatment of ItgaxCre-iDTR mice affected neither the total number nor the activation status of NK cells significantly (Figures S7C and S7D). Having thus excluded a major effect on NK cells, we analyzed the contribution of TLR9 and MyD88 signaling in individual DC subsets in regulating NK cell function and MCMV clearance. This was achieved by depleting the endogenous pool of CD11c^{+} cells in ItgaxCre-iDTR mice and reconstituting them with Flt3-L-derived cDCs or pDCs from WT, TLR9$^{-/-}$, and MyD88^{OFF} mice or both DC subsets from WT mice (termed mixed WT DCs), as shown in Figure 6A. As additional controls, we included DT-treated ItgaxCre-iDTR mice that were either transgenic (DT sensitive) or WT (DT insensitive) for Cre expression but did not receive any DCs. Adoptive transfer of WT cDCs or pDCs led to a pronounced increase in NK cell CD69 expression compared to mice that did not receive any DCs (Figure 6B). In contrast, WT cDCs were more effective at inducing IFN-γ production by NK cells than WT pDCs (Figure 6C). Simultaneously, TLR9$^{-/-}$ and MyD88^{OFF} cDCs promoted significantly less NK cell CD69 expression and IFN-γ production compared to WT cDCs, whereas pDC contribution to NK cell activation was less dependent on TLR9 signaling (Figures 6B and 6C). Besides, absence of CD11c^{+} DCs strongly reduced NK cell degranulation (Figure 6D), but this was efficiently restored by adoptive transfer of cDCs, pDCs, or a mix of both, irrespective of their expression of TLR9 and MyD88 (Figure 6D).

Given that NK cells control clearance of MCMV in vivo, we finally compared the contribution of each DC subset to viral clearance. To address this aim, we infected mice with MCMV expressing luciferase and quantified viral load using intravital imaging. Mice receiving mixed WT DCs were better at controlling MCMV infection than mice that did not receive any DCs or mixed Toll-like receptor (TLR) signaling-deficient DCs (Figure 6E). Furthermore, adoptive transfer of WT cDCs alone, but not pDCs, into DC-depleted mice restored MCMV control (Figures 6F and 6G). Again, transfer of TLR9$^{-/-}$ or MyD88^{OFF} DC subsets failed to improve MCMV clearance at day 1.5 p.i. (Figures 6E and 6G). Thus, we demonstrate that in the absence of pDCs, cDCs are

(C–E) WT NK cells were cultured with recombinant IL-12 or IL-15 in vitro. Representative dot plots (C) and quantification (D) of frequencies of IFN-γ^{+} NK cells. (E) Representative histograms of CD107a expression on NK cells.

(F) Frequencies of CD107a^{+} NK cells cultured with different concentrations of recombinant IL-15 (1, 10, or 100 ng/mL).

(G) Sorted WT pDCs and cDCs were infected with MCMV for 24 hrs. WT NK cells were cultured with supernatants of these MCMV-infected cDCs or pDCs for 24 hrs in the presence or absence of anti IL-15 antibody. Degranulation was determined as the frequency of CD107a^{+} NK cells in the culture.

(H) Representative dot plots of WT NK cell degranulation after co-culture with cDCs alone or with anti-IL-15 antibody.

(I–K) Relative expression of IL-12 (I), IL-15 (J), and IFN-β (K) mRNAs in ex vivo splenic pDCs and cDCs sorted on day 1.5 of MCMV infection.

Data are from one of two individual experiments with similar results. NS, not significant; ***$p < 0.001$, **$p < 0.01$, *$p < 0.05$; one-way ANOVA with Tukey post test.

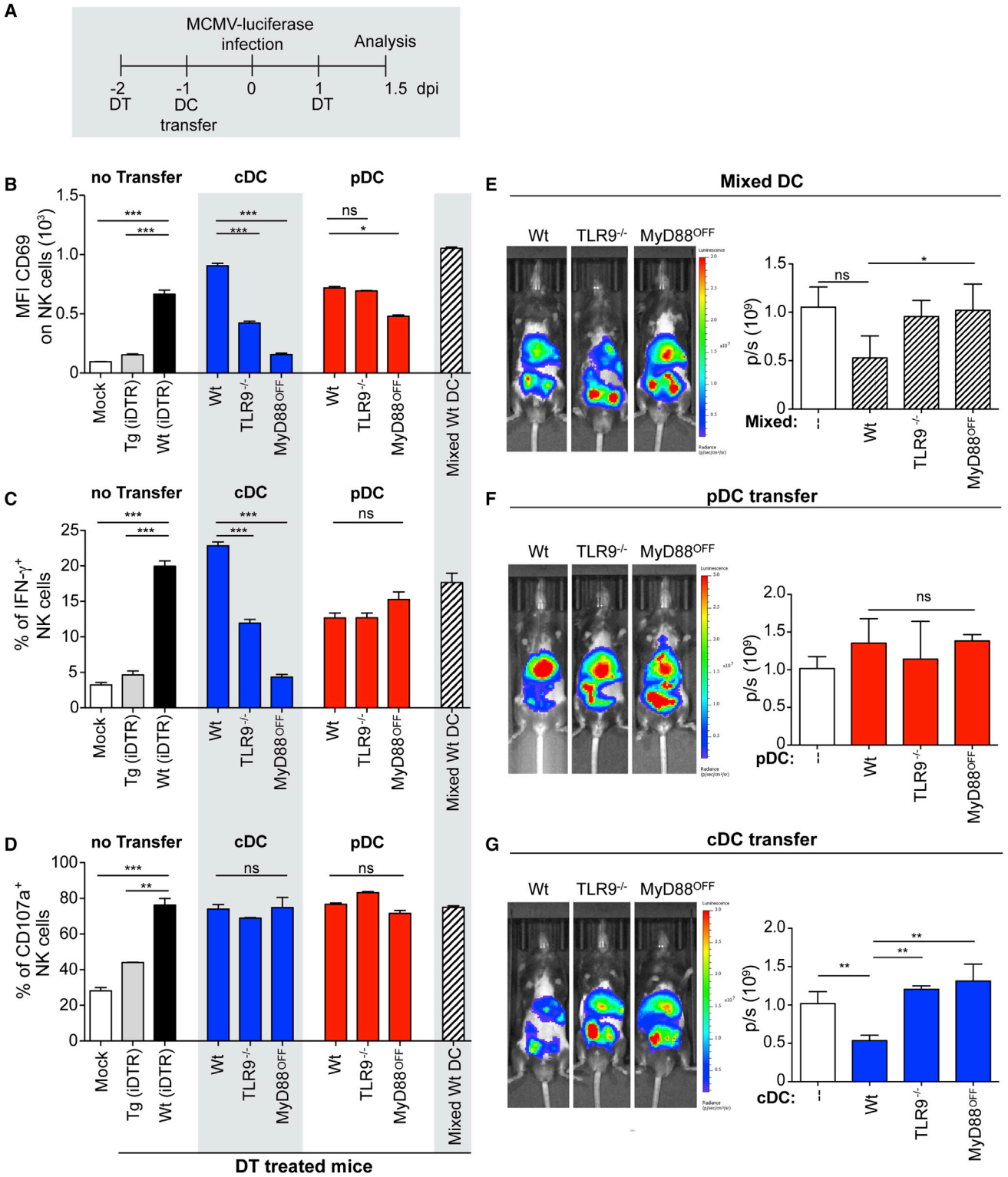

Figure 6. cDC-Derived TLR9 and MyD88 Signaling Promotes Robust NK Cell Effector Function and Efficient Viral Clearance

ItgaxCre-iDTR mice were used to evaluate the contribution of individual DC subsets in NK cell effector function and viral clearance. ItgaxCre-iDTR transgenic mice are denoted as Tg (iDTR), and WT littermate controls are denoted as WT (iDTR).

(A) Schematic overview of DC depletion strategy by DT administration followed by adoptive transfer of sorted cDCs, pDCs, or mixed DCs in DC-depleted mice later infected with 5×10^5 PFUs of MCMV.

(legend continued on next page)

able to promote efficient NK cell activation and IFN-γ production in a TLR9- and MyD88-dependent manner, while both DC subsets combine to achieve maximum clearance of MCMV infection.

DISCUSSION

TLR9 and MyD88 are of central importance to fight MCMV, because constitutive KO mice of either gene result in dramatically reduced immune protection against the virus (Delale et al., 2005; Krug et al., 2004; Tabeta et al., 2004; Zucchini et al., 2008b). These signaling pathways are found, in addition to pDCs, in a diverse range of other cell types. These include cells that are permissive for MCMV replication, such as non-hematopoietic stromal cells (Benedict et al., 2006; Hsu et al., 2009), which contain the bulk of viral infection after 3 days (Benedict et al., 2006), and to a minor extent cDCs (Dalod et al., 2003). Using BM chimeras and transgenic mice that allowed us to specifically delete TLR9 or reactivate MyD88 function in a cell type-specific manner, we show that activation of the TLR9/MyD88 signaling pathway in hematopoietic cells is sufficient to promote early viral control in the spleen, while in the liver, viral clearance is MyD88 dependent but TLR9 independent. In contrast, TLR9 signaling within the non-hematopoietic compartment did not contribute to viral clearance at day 1.5 p.i. Our results further demonstrate that within the hematopoietic compartment, TLR9/MyD88 expression in $CD11c^+$ DCs, but not in $LysM^+$ macrophages, is required to control MCMV infection and to sustain systemic IL-12p40 and IFN-I production.

Sensing of MCMV by DCs is vital for protective immunity, mainly due to their cross-talk with NK cells (Degli-Esposti and Smyth, 2005). For example, in mice with reduced DC numbers, anti-viral NK cell function in the spleen has been shown to be compromised (Andoniou et al., 2005; Andrews et al., 2003; Mitrović et al., 2012; Robbins et al., 2007). NK cells confer immunity against MCMV through the production of inflammatory cytokines such as IFN-γ and by direct killing of infected cells (Bukowski et al., 1984). Here we show that at day 1.5 p.i., TLR9 and MyD88 signaling in $CD11c^+$ DCs is required for NK cell contraction, CD69 expression, and IFN-γ production, suggesting an essential role for these pathways in coordinating ensuing immune responses against MCMV.

Early DC-NK cell interaction is regulated by various pro-inflammatory cytokines. Among them, IL-12 has been shown to elevate IFN-γ secretion by NK cells, while IFN-I and IL-15 have been described to trigger NK cell cytotoxicity, proliferation, and survival (Baranek et al., 2012; Nguyen et al., 2002; Orange and Biron, 1996b). The first short-lived peak of IFN-I production after systemic MCMV infection at 8 hr p.i. is mainly stromal cell derived (Schneider et al., 2008), while the second, more sustained peak from day 1.5 p.i. is pDC dependent (Dalod et al., 2002). Consistent with this, in our study, reactivation of MyD88 signaling exclusively in pDCs significantly restores IFN-I levels at day 1.5 p.i. compared to $MyD88^{OFF}$ mice. However, MyD88 signaling only in pDCs has a negligible impact on NK cell function and viral clearance. In accordance, previous reports using experimental ablation of pDCs in vivo suggest that this DC subset is dispensable for NK cell activation (Dalod et al., 2002; Krug et al., 2004; Swiecki et al., 2010). Although in our experimental settings only a fraction of pDCs reactivates MyD88 (approximately 30%), our results using reconstitution of specific DC populations upon total DC ablation in ItgaxCre-iDTR mice further support the notion that pDCs alone may not be sufficient for anti-MCMV immunity. Moreover, although NK cell cytotoxicity was thought to be strongly influenced by IFN-β induced after infection (Steinberg et al., 2009), our results suggest that loss of IFN-α and IFN-β in $IRF7^{-/-}$IFN-$\beta^{\Delta/\Delta}$ mice or complete loss of IFN-I signaling in IFNAR-$1^{-/-}$ mice has no influence on NK cell degranulation and cytotoxicity. Altogether, these data suggest that alternative signals, other than pDC-derived IFN-I, may promote effector NK cell cytotoxic activity in TLR9/MyD88-deficient mice.

Previous studies alluded to an important role for cDCs in promoting NK cell activation and/or virus control during MCMV infection (Andoniou et al., 2005; Andrews et al., 2003; Asselin-Paturel et al., 2001; Baranek et al., 2012; Delale et al., 2005; Swiecki et al., 2010; Zucchini et al., 2008a). However, we demonstrate that TLR9 and MyD88 mechanisms in cDCs alone are able to intercede in the absence of pDCs to promote robust NK cell function and viral clearance in infected mice. This finding can be understood in light of a previous report showing that pDC-derived IFN-I impairs IL-12 production by splenic cDCs in a signal transducer and activator of transcription 1 (STAT-1)-dependent manner (Dalod et al., 2002). Therefore, in the absence of IFN-I from pDCs, an over-production of IL-12 by cDCs (Dalod et al., 2002; Krug et al., 2004; Swiecki et al., 2010) may efficiently generate effector NK cell function. We found that IL-12 alone, which is mainly derived from cDCs, can robustly induce IFN-γ secretion from NK cells.

Consistent with previous studies (Cocita et al., 2015; Madera and Sun, 2015; Nabekura et al., 2015), we propose that MyD88 expression in NK cells is required exclusively to transduce DC-derived IL-1 family cytokine signals, because induction of IFN-γ production in MyD88-deficient NK cells induced by MCMV-infected WT DCs was reduced compared to WT or TLR9-deficient NK cells. Besides the effects of IL-12 on NK cell activation, cDC-derived IL-15 strongly boosts NK cell degranulation. Altogether, our data indicate that the presence of TLR9 and MyD88 signaling in cDCs allows adequate NK cell function and early MCMV clearance. In this respect, our study introduces an interesting concept, because it is generally assumed that during many viral infections, including MCMV infection, the primary function of TLR9 and MyD88 signaling is to promote high systemic levels of IFN-I by pDCs, with a lesser, if any, role in the direct activation of cDCs.

We also demonstrate that cDC-derived TLR9 and MyD88 signaling affects only the early cytokine-dependent NK cell

(B–D) MFI of CD69 expression (B), percentage of $IFN\text{-}\gamma^+$ (C), and percentage of $CD107a^+$ splenic NK cells (D) at day 1.5 p.i.
(E–G) Mice were infected with MCMV-luciferase at 5×10^5 PFUs, and viral clearance was evaluated by intravital imaging after adoptive transfer of mixed DCs (E), sorted pDCs (F), and sorted cDCs (G).
Data are from one of three individual experiments with similar results. n = 3–5 mice/group; means ± SD; NS, not significant; ***$p < 0.001$, **$p < 0.01$, *$p < 0.05$; one-way ANOVA with Tukey post test.

activation at day 1.5 p.i., while the expansion of Ly49H$^+$ NK cells at day 8 p.i. remains unchanged. This correlates with previous reports in which Ly49H$^+$ NK cells from BALB/c-Ly49H$^+$MyD88$^{-/-}$ mice display minimal changes in expansion and activation compared to NK cells from BALB/c-Ly49H$^+$ mice at days 3 and 6 p.i. (Cocita et al., 2015). Similarly, Geurs et al. (2009) showed that the engagement of Ly49H receptor in C57BL/6 mice was able to compensate for the loss of early cytokine stimulation, and by day 3 p.i., Ly49H$^+$ NK cells expanded comparably to WT mice in the absence of IFN-I.

In summary, by generating valuable genetic tools, we were able to reconstruct the chain of events occurring early upon systemic MCMV infection. We show that MCMV clearance is dependent on TLR9 and MyD88 signaling from hematopoietic cells. CD11c$^+$ cDCs are fundamental in initiating protective immunity against MCMV, and in the absence of cDCs, MCMV clearance and NK cell function are significantly impaired. Specifically, cDCs control independent arms of NK cell function during acute MCMV infection by driving NK cell IFN-γ and acquisition of cytotoxic granules via IL-12 and IL-15, respectively. Our data explain mechanistically why depletion of CD11c$^+$ DCs significantly increases the viral load in primary organs, as recently demonstrated (Holzki et al., 2015). Altogether, our results show that in the absence of pDCs, TLR9 and MyD88 signaling in cDCs is mandatory for MCMV clearance and NK cell effector function during the early phase of MCMV infection. Overall, our data provide a paradigm shift in understanding the importance of cDCs in early MCMV immunity by demonstrating that direct activation of cDCs via TLR9 and MyD88 is sufficient to ensure adequate antiviral immune responses after acute MCMV infection.

EXPERIMENTAL PROCEDURES

Ethics Statement

All animal experiments were performed as per the German animal protection law (TierSchG BGBl. I S. 1105; 25.05.1998). The housing and handling of mice was set by the regulations of the Federation of European of Laboratory Animal Science Associations (FELASA) and the national animal welfare body of the Gesellschaft für Versuchstierkunde/Society of Laboratory Animal Science (GV-SOLAS). All animal experiments were approved by the Lower Saxony Committee on the Ethics of Animal Experiments, as well as the responsible state office (Lower Saxony State Office of Consumer Protection and Food Safety), under permits 33.9-42502-04-12/1020 and 33.9-42502-04-09/1785. Surgery of mice was performed following euthanasia in a CO_2 chamber in accordance to the German animal welfare law. All efforts were made to minimize suffering.

Mice

All mouse lines were bred at the animal facility of Twincore (Hannover, Germany) or at the Helmholtz Centre for Infection Research (HZI, Braunschweig, Germany) under specific pathogen-free conditions. Mice between 6 and 12 weeks of age were used for experiments. Among the mouse lines used in our study, TLR9$^{-/-}$ mice were provided by Shizuo Akira (Hemmi et al., 2000), MyD88^{OFF} mice were provided by Bernard Holzmann (Gais et al., 2012), RFP mice were provided by Hans Jörg Fehling (Luche et al., 2007), ItgaxCre mice were provided by Boris Reizis (Caton et al., 2007), LysM-Cre mice were provided by Irmgard Förster (Clausen et al., 1999), IRF7$^{-/-}$ mice were provided by Tadatsugu Taniguchi (Honda et al., 2005), IFN-$\beta^{WT/\Delta}$ mice were provided by S.L. (Lienenklaus et al., 2009), iDTR mice were provided by Ari Waisman (Buch et al., 2005), and IFNAR-1$^{-/-}$ mice were provided by Till Strowig (Müller et al., 1994). All mice were raised on a C57BL/6J background.

Generation of TLR9$^{fl/fl}$ Mice

Exon 2, comprising the major coding sequence of the *Tlr9* gene, was flanked by loxP sites to generate TLR9$^{fl/fl}$ mice. The targeting vector consisted of a loxP site downstream of exon 1 followed by a FRT-flanked neomycin resistance gene upstream of exon 2. An additional F3-flanked puromycin resistance cassette was inserted following exon 2 to increase co-recombination frequency of both loxP sites. The targeting vector was also composed of an ampicillin resistance gene and herpes simplex virus thymidine kinase (Tk) gene driven by a phosphoglycerate kinase (pgk) promoter. The targeting vector was linearized with *Not* I and transfected into C57BL/6N embryonic stem cells (ESCs) by electroporation. G418 and ganciclovir-resistant ESCs were selected as correctly targeted colonies and underwent Southern blot analysis. The TLR9$^{fl/fl}$ mice were next backcrossed with C57BL/6J mice for at least ten generations before being used in experiments. TLR9$^{fl/fl}$ mice were then crossed to cell-specific Cre recombinase-expressing mouse lines to allow Cre-mediated deletion of exon 2 and subsequent removal of most of the open reading frame of the *Tlr9* gene (Figure S1A). Hence, using this approach, mice with cell-specific loss of TLR9 function in Cre recombinase-expressing cells were obtained. The TLR9$^{fl/fl}$ mice were generated by Taconic Artemis as part of a collaboration initiated by H.W. and T.S.

Generation of BM Chimeric Mice

BM chimeric mice were generated as previously described (Dudek et al., 2016).

MCMV Viral Strains

bacterial artificial chromosome (BAC)-derived MCMV (Jordan et al., 2011) and luciferase-expressing MCMV strains were provided by L.C.-S. and used for infection experiments. Propagation of MCMV stocks was carried out as previously described (Lindenberg et al., 2014).

Generation of MCMV-Δie2-luc

For the generation of MCMV-luciferase, the firefly luciferase cassette of the pGL3 plasmid (Promega) was inserted into the pcDNA3.1 plasmid (Life Technologies) using the restriction enzymes HindIII and XbaI, thereby adding the bovine growth hormone (BGH) poly(A) region to the luciferase cassette. In the following step, the ie2 gene of the MCMV BAC (Smith strain, repaired MCK-2) (Jordan et al., 2011) was replaced with the luciferase-BGH poly(A) cassette via en passant mutagenesis (Tischer et al., 2010). The start codon of the luciferase gene is in the exact position of the start codon of the ie2 gene, creating an MCMV virus lacking the ie2 gene with luciferase driven by the major immediate early promoter (MIEP).

In Vivo Systemic Infection

Mice were either infected intraperitoneally (i.p.) with 5×10^5 plaque-forming units (PFUs) of the MCMV-Smith strain, MCMV-luciferase, or were mock-infected with PBS. For MCMV-luciferase-infected mice, images were quantified at days 1.5, 3, 6, and 8 p.i. For NK cell analysis, spleens were harvested at days 1.5 and 8 p.i., and virus concentration was determined in the spleen and liver at day 1.5 p.i.

MCMV Quantification by Plaque Assay

Spleen and liver were harvested from day 1.5 p.i. mice and collected in 0.5 mL DMEM. Virus titers in the infected organs were quantified as described previously (Lindenberg et al., 2014).

In Vitro MCMV Spin Infection

Flow cytometry-sorted Flt3-L-derived pDCs and cDCs were seeded at 1×10^5 cells/well in a 96-well U-bottom plate. DCs were treated with MCMV (MOI 2), 1 μM CpG, or PBS for 24 hrs. DC infection was performed by centrifugation at 1,500 rpm for 30 min at 37°C and later incubated at 37°C, 5% CO_2, for 24 hrs.

Generation of Flt3-L-Differentiated BM DCs

Tibiae and femurs from mice were harvested, and BM was isolated. BM DCs comprising pDCs and cDCs were generated by in vitro differentiation with Flt3-L as previously described (Naik et al., 2010).

Flow Cytometry

Cells were washed in PBS and stained with the live/dead fixable aqua dead cell stain kit (Invitrogen) to exclude dead cells. Cells were further processed for staining as previously described (Puttur et al., 2013).

Antibodies

In this study, all antibodies used were purchased from eBioscience unless stated otherwise. The following fluorochrome-labeled anti-mouse antibodies were used. For DCs after in vitro infection, B220 (RA3-6B2), CD11c (N418), CD86 (GL1), MHCII (AF6-120.1), and CD8α (53–6.7) were used. For splenic NK cells, NK 1.1 (PK136), Ly49H (3D10), CD69 (H1.2F3), CD3ε (145-2C11), and CD107a (eBio1D4B) antibodies were stained extracellularly. IFN-γ (XMG1.2) staining was performed by intracellular staining. For IL-15 neutralization, goat anti-mouse IL-15 antigen affinity-purified polyclonal antibody from R&D Systems was used.

Cell Sorting

Cell sorting was carried out at the Cell Sorting Core facility of the Hannover Medical School using the FACSAria (BD Biosciences), XDP or MoFlo (Beckman Coulter) fluorescence-activated cell sorting (FACS) machines. In vitro differentiated or ex vivo pDCs were sorted as $CD11c^{int}B220^{+}$, cDCs were sorted as $CD11c^{hi}B220^{-}$, and NK cells were sorted as $NK1.1^{+}CD3^{-}$ from spleens. Cells were processed as previously described (Puttur et al., 2013).

Isolation of Splenic NK Cells

Spleens were cut into small pieces and mechanically homogenized in RPMI 1640 Glutamax medium (Gibco) supplemented with 10% fetal calf serum (FCS), 5 μM β-mercaptoethanol (Gibco), and 100 U/mL penicillin/streptomycin (Biochrom). A single-cell suspension was prepared, and red blood cells (RBCs) were lyzed in RBC lysis buffer (150 mM NH_4Cl, 10 mM $KHCO_3$, and 0.1 mM EDTA). The isolated cells were counted by trypan blue dead cell exclusion method, and live cells were adjusted to the same cell number for flow cytometry staining.

In Vitro NK Cell Stimulation

Sorted NK cells were stimulated for 24 hrs in the presence of cDCs and/or pDCs at 1:1 ratio, recombinant murine IL-12 (100 ng/mL) from PeproTech, recombinant murine IL-15 (1, 10, or 100 ng/mL) from PeproTech, 1 μM CpG, or MCMV (MOI 2). In the last 6 hr, IL-2 (800 U/mL) and brefeldin A (3 μg/mL) were added; later, the cells were stained for intracellular IFN-γ.

NK Cell Degranulation Assay

Ex vivo isolated and sorted day 1.5 MCMV-infected splenic NK effector (E) cells were cultured in the presence of YAC-1 target (T) cells. YAC-1 cells were provided by R.J. NK cells at a concentration of 1×10^5 cells/well and were co-cultivated with YAC-1 cells at E:T ratios of 5:1, 2.5:1, and 1:1 in a 96-well V-bottom plate in the presence of anti-CD107a (eBio1D4B) antibody at a final concentration of 0.01 mg/mL at 37°C, 5% CO_2. Following 1 hr of incubation, monensin (BD Biosciences) was added to inhibit endosomal acidification at a final concentration of 5 mg/mL, and incubation was continued for an additional 3 hr as described previously (Marquardt et al., 2010). After a 4 hr incubation period, cells were stained and analyzed by flow cytometry.

NK Cell Chromium Release Assay

Splenic NK cells were sorted on day 1.5 p.i. and pre-activated with IL-2 for 2 hr. Activated NK cells were then co-cultured with YAC-1 target cells that were labeled with 1 mCi/mL ^{51}Cr for 2 hr at an E:T ratios of 5:1 and 2.5:1 in a 96-well V-bottom plate. Effector and target cells were co-cultured at 37°C for 4 hr, and Cr-release assay was performed by the R.J. lab as described earlier (Jacobs et al., 1992).

Cytokine Quantification

Supernatants from in vitro-stimulated sorted cDCs, pDCs, or serum and organ homogenate samples from MCMV-infected mice were used to determine cytokine concentration by ELISA as previously described (Puttur et al., 2013).

Immunofluorescence

Cryo sections (5 μm) of snap-frozen lung tissue were fixed before incubation with anti-NKp46 (R&D Systems). After serum block (Dianova), sections were incubated with Alexa 488-labeled anti-goat (Invitrogen) followed by incubation with anti-RFP (Antibodies Online). RFP antibody was detected by Alexa 555-labeled anti-rabbit (Invitrogen), and nuclei were stained using DAPI (Sigma). Sections were placed on coverslips with Fluoromount G (eBioscience), and images were acquired using the AxioImager Z1 microscope (Carl Zeiss). All evaluations were performed in a blinded manner.

In Vivo Imaging

Mice infected with MCMV-luciferase were anesthetized in a chamber supplied with isoflurane 2% O_2. IVIS Spectrum computed tomography (CT) (PerkinElmer) was used for imaging, and further analysis was performed using Living Image v.4.3.1 software (PerkinElmer). Luciferin was administered i.p. in 100 μL, 2 min before analysis. Mice were placed in an imaging platform, and whole-body images were taken at a binning factor of 8 over 5 s to 1 min at the indicated time points during infection. Luminescence emitted from the region of interest in each mouse was quantified as total flux and pseudo-color images representing intensity from virus-derived luminescence were generated. For detection of three-dimensional bioluminescent signals, anesthetized mice were first scanned by CT under the mode of medium resolution and then MCMV-derived bioluminescent signals were excited under the wavelength firefly 612 nm and imaged at a binning factor of 8 over 5 s to 1 min.

RNA Isolation and Real-Time qPCR

RNA from spleens and FACS-sorted pDCs and cDCs were isolated as per instructions using the RNeasy Micro Kit (QIAGEN). Cells were lyzed in RLT buffer with 0.01% β-mercapthanol. The cell lysate was placed in MinElute spin columns with 70% ethanol. The samples were treated with DNase for 15 min and inactivated with RW1 buffer. After washing, purified RNA was eluted in 14 μL of RNase-free water.

The following primers were used: *β-actin* forward strand 5′-TGTTACCA ACTGGGACGACA-3′, reverse strand 5′-GGGGTGTTGAAGGTCTCAAA-3′; *TLR9* forward strand 5′-CCAGACGCTCTTCGAGAACC-3′; reverse strand 5′-GTTATAGAAGTGGCGGTTGT-3′; and *Myd88* forward strand 5′-AGAGCTG CTGGCCTTGTTAG-3′, reverse strand 5′-TTCTCGGACTCCTGGTTCTG-3′. Primers were obtained from Eurofins MWG Operon and were analyzed on a LightCycler 480 II (Roche). Relative gene expression was calculated as $[2^{-Ct(target)}/2^{-Ct(\beta\text{-Actin})}]$.

Statistics

The unpaired Student's t test, one-way ANOVA, and the Kruskal-Wallis test were used to calculate the statistically significant differences between samples. A value for $p < 0.05$ was considered significant, as indicated by an asterisk sign: *$p < 0.05$, **$p < 0.01$, and ***$p < 0.001$.

SUPPLEMENTAL INFORMATION

Supplemental Information includes seven figures and can be found with this article online at http://dx.doi.org/10.1016/j.celrep.2016.09.055.

AUTHOR CONTRIBUTIONS

F.P. and M.F. designed the experiments. F.P., M.F., G.S., C.B., M.L., M.G., and M.S. performed the experiments. L. Bo and L.C.-S. provided the MCMV stocks. D.T. and R.J. performed the NK cytotoxicity experiments. A.A.K. performed and provided the immunofluorescence data. S.L. provided the $IRF7^{-/-}$ mice. B.H. provided the $MyD88^{OFF}$ mice. H.W., L.B., and T.S., in collaboration with Taconic Artemis, generated the $TLR9^{fl/fl}$ mice. M.F. and F.P. analyzed the data and prepared the figures. F.P. and T.S. supervised the work. F.P., L. Berod and T.S. wrote the manuscript.

ACKNOWLEDGMENTS

We acknowledge Taconic Artemis for generating the $TLR9^{fl/fl}$ mice in collaboration with H.W. and T.S. We thank Friederike Kruse for expert technical assistance and Lucía Minarrieta and Peyman Ghorbani for critical reading of the manuscript. In addition, we thank Dr. Till Strowig for the $IFNAR\text{-}1^{-/-}$ mice

and Dr. Tobias May for providing us with the Dox-MEF cell lines. We acknowledge the assistance of the Cell Sorting Core Facility of the Hannover Medical School, supported in part by Braukmann-Wittenberg-Herz-Stiftung and Deutsche Forschungsgemeinschaft. F.P. was supported by the HiLF foundation provided by the Hannover Medical School (MHH). M.F. was supported by the fellowship Ciências sem Fronteiras/DAAD. C.B. was supported by the European Molecular Biology Organization (EMBO). L.B. is supported by the Ellen-Schmidt Program from the MHH. Finally, we acknowledge the Deutsche Forschungsgemeinschaft SFB 900 (Sonderforschungsbereich 900) and the HiLF grant funding body for providing the financial resources to carry out this study.

Received: June 26, 2016
Revised: August 9, 2016
Accepted: September 16, 2016
Published: October 18, 2016

REFERENCES

Ahmed, A. (2011). Antiviral treatment of cytomegalovirus infection. Infect. Disord. Drug Targets *11*, 475–503.

Alexandre, Y.O., Cocita, C.D., Ghilas, S., and Dalod, M. (2014). Deciphering the role of DC subsets in MCMV infection to better understand immune protection against viral infections. Front Microbiol *5*, 378.

Andoniou, C.E., van Dommelen, S.L., Voigt, V., Andrews, D.M., Brizard, G., Asselin-Paturel, C., Delale, T., Stacey, K.J., Trinchieri, G., and Degli-Esposti, M.A. (2005). Interaction between conventional dendritic cells and natural killer cells is integral to the activation of effective antiviral immunity. Nat. Immunol. *6*, 1011–1019.

Andrews, D.M., Scalzo, A.A., Yokoyama, W.M., Smyth, M.J., and Degli-Esposti, M.A. (2003). Functional interactions between dendritic cells and NK cells during viral infection. Nat. Immunol. *4*, 175–181.

Arnold-Schrauf, C., Dudek, M., Dielmann, A., Pace, L., Swallow, M., Kruse, F., Kühl, A.A., Holzmann, B., Berod, L., and Sparwasser, T. (2014). Dendritic cells coordinate innate immunity via MyD88 signaling to control *Listeria monocytogenes* infection. Cell Rep. *6*, 698–708.

Arnold-Schrauf, C., Berod, L., and Sparwasser, T. (2015). Dendritic cell specific targeting of MyD88 signalling pathways in vivo. Eur. J. Immunol. *45*, 32–39.

Asselin-Paturel, C., Boonstra, A., Dalod, M., Durand, I., Yessaad, N., Dezutter-Dambuyant, C., Vicari, A., O'Garra, A., Biron, C., Brière, F., and Trinchieri, G. (2001). Mouse type I IFN-producing cells are immature APCs with plasmacytoid morphology. Nat. Immunol. *2*, 1144–1150.

Baranek, T., Manh, T.P., Alexandre, Y., Maqbool, M.A., Cabeza, J.Z., Tomasello, E., Crozat, K., Bessou, G., Zucchini, N., Robbins, S.H., et al. (2012). Differential responses of immune cells to type I interferon contribute to host resistance to viral infection. Cell Host Microbe *12*, 571–584.

Benedict, C.A., De Trez, C., Schneider, K., Ha, S., Patterson, G., and Ware, C.F. (2006). Specific remodeling of splenic architecture by cytomegalovirus. PLoS Pathog. *2*, e16.

Berod, L., Stüve, P., Swallow, M., Arnold-Schrauf, C., Kruse, F., Gentilini, M.V., Freitag, J., Holzmann, B., and Sparwasser, T. (2014). MyD88 signalling in myeloid cells is sufficient to prevent chronic mycobacterial infection. Eur. J. Immunol. *44*, 1399–1409.

Buch, T., Heppner, F.L., Tertilt, C., Heinen, T.J., Kremer, M., Wunderlich, F.T., Jung, S., and Waisman, A. (2005). A Cre-inducible diphtheria toxin receptor mediates cell lineage ablation after toxin administration. Nat. Methods *2*, 419–426.

Bukowski, J.F., Woda, B.A., and Welsh, R.M. (1984). Pathogenesis of murine cytomegalovirus infection in natural killer cell-depleted mice. J. Virol. *52*, 119–128.

Caton, M.L., Smith-Raska, M.R., and Reizis, B. (2007). Notch-RBP-J signaling controls the homeostasis of CD8− dendritic cells in the spleen. J. Exp. Med. *204*, 1653–1664.

Clausen, B.E., Burkhardt, C., Reith, W., Renkawitz, R., and Förster, I. (1999). Conditional gene targeting in macrophages and granulocytes using LysMcre mice. Transgenic Res. *8*, 265–277.

Cocita, C., Guiton, R., Bessou, G., Chasson, L., Boyron, M., Crozat, K., and Dalod, M. (2015). Natural killer cell sensing of infected cells compensates for MyD88 deficiency but not IFN-I activity in resistance to mouse cytomegalovirus. PLoS Pathog. *11*, e1004897.

Dalod, M., Salazar-Mather, T.P., Malmgaard, L., Lewis, C., Asselin-Paturel, C., Brière, F., Trinchieri, G., and Biron, C.A. (2002). Interferon alpha/beta and interleukin 12 responses to viral infections: pathways regulating dendritic cell cytokine expression in vivo. J. Exp. Med. *195*, 517–528.

Dalod, M., Hamilton, T., Salomon, R., Salazar-Mather, T.P., Henry, S.C., Hamilton, J.D., and Biron, C.A. (2003). Dendritic cell responses to early murine cytomegalovirus infection: subset functional specialization and differential regulation by interferon alpha/beta. J. Exp. Med. *197*, 885–898.

Degli-Esposti, M.A., and Smyth, M.J. (2005). Close encounters of different kinds: dendritic cells and NK cells take centre stage. Nat. Rev. Immunol. *5*, 112–124.

Delale, T., Paquin, A., Asselin-Paturel, C., Dalod, M., Brizard, G., Bates, E.E., Kastner, P., Chan, S., Akira, S., Vicari, A., et al. (2005). MyD88-dependent and -independent murine cytomegalovirus sensing for IFN-alpha release and initiation of immune responses in vivo. J. Immunol. *175*, 6723–6732.

Dokun, A.O., Chu, D.T., Yang, L., Bendelac, A.S., and Yokoyama, W.M. (2001). Analysis of in situ NK cell responses during viral infection. J. Immunol. *167*, 5286–5293.

Dudek, M., Puttur, F., Arnold-Schrauf, C., Kuhl, A.A., Holzmann, B., Henriques-Normark, B., Berod, L., and Sparwasser, T. (2016). Lung epithelium and myeloid cells cooperate to clear acute pneumococcal infection. Mucosal Immunol. *9*, 1288–1302.

Gais, P., Reim, D., Jusek, G., Rossmann-Bloeck, T., Weighardt, H., Pfeffer, K., Altmayr, F., Janssen, K.P., and Holzmann, B. (2012). Cutting edge: divergent cell-specific functions of MyD88 for inflammatory responses and organ injury in septic peritonitis. J. Immunol. *188*, 5833–5837.

Geurs, T.L., Zhao, Y.M., Hill, E.B., and French, A.R. (2009). Ly49H engagement compensates for the absence of type I interferon signaling in stimulating NK cell proliferation during murine cytomegalovirus infection. J. Immunol. *183*, 5830–5836.

Hemmi, H., Takeuchi, O., Kawai, T., Kaisho, T., Sato, S., Sanjo, H., Matsumoto, M., Hoshino, K., Wagner, H., Takeda, K., and Akira, S. (2000). A Toll-like receptor recognizes bacterial DNA. Nature *408*, 740–745.

Holzki, J.K., Dağ, F., Dekhtiarenko, I., Rand, U., Casalegno-Garduño, R., Trittel, S., May, T., Riese, P., and Čičin-Šain, L. (2015). Type I interferon released by myeloid dendritic cells reversibly impairs cytomegalovirus replication by inhibiting immediate early gene expression. J. Virol. *89*, 9886–9895.

Honda, K., Yanai, H., Negishi, H., Asagiri, M., Sato, M., Mizutani, T., Shimada, N., Ohba, Y., Takaoka, A., Yoshida, N., and Taniguchi, T. (2005). IRF-7 is the master regulator of type-I interferon-dependent immune responses. Nature *434*, 772–777.

Hsu, K.M., Pratt, J.R., Akers, W.J., Achilefu, S.I., and Yokoyama, W.M. (2009). Murine cytomegalovirus displays selective infection of cells within hours after systemic administration. J. Gen. Virol. *90*, 33–43.

Jacobs, R., Stoll, M., Stratmann, G., Leo, R., Link, H., and Schmidt, R.E. (1992). CD16− CD56+ natural killer cells after bone marrow transplantation. Blood *79*, 3239–3244.

Jordan, S., Krause, J., Prager, A., Mitrovic, M., Jonjic, S., Koszinowski, U.H., and Adler, B. (2011). Virus progeny of murine cytomegalovirus bacterial artificial chromosome pSM3fr show reduced growth in salivary glands due to a fixed mutation of MCK-2. J. Virol. *85*, 10346–10353.

Krmpotic, A., Bubic, I., Polic, B., Lucin, P., and Jonjic, S. (2003). Pathogenesis of murine cytomegalovirus infection. Microbes Infect. *5*, 1263–1277.

Krug, A., French, A.R., Barchet, W., Fischer, J.A., Dzionek, A., Pingel, J.T., Orihuela, M.M., Akira, S., Yokoyama, W.M., and Colonna, M. (2004). TLR9-dependent recognition of MCMV by IPC and DC generates coordinated

cytokine responses that activate antiviral NK cell function. Immunity *21*, 107–119.

Lienenklaus, S., Cornitescu, M., Zietara, N., Łyszkiewicz, M., Gekara, N., Jabłónska, J., Edenhofer, F., Rajewsky, K., Bruder, D., Hafner, M., et al. (2009). Novel reporter mouse reveals constitutive and inflammatory expression of IFN-beta in vivo. J. Immunol. *183*, 3229–3236.

Lindenberg, M., Solmaz, G., Puttur, F., and Sparwasser, T. (2014). Mouse cytomegalovirus infection overrules T regulatory cell suppression on natural killer cells. Virol. J. *11*, 145.

Lodoen, M.B., and Lanier, L.L. (2006). Natural killer cells as an initial defense against pathogens. Curr. Opin. Immunol. *18*, 391–398.

Luche, H., Weber, O., Nageswara Rao, T., Blum, C., and Fehling, H.J. (2007). Faithful activation of an extra-bright red fluorescent protein in "knock-in" Cre-reporter mice ideally suited for lineage tracing studies. Eur. J. Immunol. *37*, 43–53.

Madera, S., and Sun, J.C. (2015). Cutting edge: stage-specific requirement of IL-18 for antiviral NK cell expansion. J. Immunol. *194*, 1408–1412.

Marquardt, N., Wilk, E., Pokoyski, C., Schmidt, R.E., and Jacobs, R. (2010). Murine CXCR3+CD27bright NK cells resemble the human CD56bright NK-cell population. Eur. J. Immunol. *40*, 1428–1439.

Min-Oo, G., and Lanier, L.L. (2014). Cytomegalovirus generates long-lived antigen-specific NK cells with diminished bystander activation to heterologous infection. J. Exp. Med. *211*, 2669–2680.

Mitrović, M., Arapović, J., Jordan, S., Fodil-Cornu, N., Ebert, S., Vidal, S.M., Krmpotić, A., Reddehase, M.J., and Jonjić, S. (2012). The NK cell response to mouse cytomegalovirus infection affects the level and kinetics of the early CD8(+) T-cell response. J. Virol. *86*, 2165–2175.

Müller, U., Steinhoff, U., Reis, L.F., Hemmi, S., Pavlovic, J., Zinkernagel, R.M., and Aguet, M. (1994). Functional role of type I and type II interferons in antiviral defense. Science *264*, 1918–1921.

Nabekura, T., Girard, J.P., and Lanier, L.L. (2015). IL-33 receptor ST2 amplifies the expansion of NK cells and enhances host defense during mouse cytomegalovirus infection. J. Immunol. *194*, 5948–5952.

Naik, S.H., O'Keeffe, M., Proietto, A., Shortman, H.H., and Wu, L. (2010). CD8+, CD8−, and plasmacytoid dendritic cell generation in vitro using flt3 ligand. Methods Mol. Biol. *595*, 167–176.

Nguyen, K.B., Salazar-Mather, T.P., Dalod, M.Y., Van Deusen, J.B., Wei, X.Q., Liew, F.Y., Caligiuri, M.A., Durbin, J.E., and Biron, C.A. (2002). Coordinated and distinct roles for IFN-alpha beta, IL-12, and IL-15 regulation of NK cell responses to viral infection. J. Immunol. *169*, 4279–4287.

Orange, J.S., and Biron, C.A. (1996a). An absolute and restricted requirement for IL-12 in natural killer cell IFN-gamma production and antiviral defense. Studies of natural killer and T cell responses in contrasting viral infections. J. Immunol. *156*, 1138–1142.

Orange, J.S., and Biron, C.A. (1996b). Characterization of early IL-12, IFN-alphabeta, and TNF effects on antiviral state and NK cell responses during murine cytomegalovirus infection. J. Immunol. *156*, 4746–4756.

Pien, G.C., Satoskar, A.R., Takeda, K., Akira, S., and Biron, C.A. (2000). Cutting edge: selective IL-18 requirements for induction of compartmental IFN-gamma responses during viral infection. J. Immunol. *165*, 4787–4791.

Plotkin, S. (2015). The history of vaccination against cytomegalovirus. Med. Microbiol. Immunol. (Berl.) *204*, 247–254.

Puttur, F., Arnold-Schrauf, C., Lahl, K., Solmaz, G., Lindenberg, M., Mayer, C.T., Gohmert, M., Swallow, M., van Helt, C., Schmitt, H., et al. (2013). Absence of Siglec-H in MCMV infection elevates interferon alpha production but does not enhance viral clearance. PLoS Pathog. *9*, e1003648.

Robbins, S.H., Tessmer, M.S., Mikayama, T., and Brossay, L. (2004). Expansion and contraction of the NK cell compartment in response to murine cytomegalovirus infection. J. Immunol. *173*, 259–266.

Robbins, S.H., Bessou, G., Cornillon, A., Zucchini, N., Rupp, B., Ruzsics, Z., Sacher, T., Tomasello, E., Vivier, E., Koszinowski, U.H., and Dalod, M. (2007). Natural killer cells promote early CD8 T cell responses against cytomegalovirus. PLoS Pathog. *3*, e123.

Scheu, S., Dresing, P., and Locksley, R.M. (2008). Visualization of IFNbeta production by plasmacytoid versus conventional dendritic cells under specific stimulation conditions in vivo. Proc. Natl. Acad. Sci. USA *105*, 20416–20421.

Schlub, T.E., Sun, J.C., Walton, S.M., Robbins, S.H., Pinto, A.K., Munks, M.W., Hill, A.B., Brossay, L., Oxenius, A., and Davenport, M.P. (2011). Comparing the kinetics of NK cells, CD4, and CD8 T cells in murine cytomegalovirus infection. J. Immunol. *187*, 1385–1392.

Schneider, K., Loewendorf, A., De Trez, C., Fulton, J., Rhode, A., Shumway, H., Ha, S., Patterson, G., Pfeffer, K., Nedospasov, S.A., et al. (2008). Lymphotoxin-mediated crosstalk between B cells and splenic stroma promotes the initial type I interferon response to cytomegalovirus. Cell Host Microbe *3*, 67–76.

Stacey, M.A., Marsden, M., Wang, E.C., Wilkinson, G.W., and Humphreys, I.R. (2011). IL-10 restricts activation-induced death of NK cells during acute murine cytomegalovirus infection. J. Immunol. *187*, 2944–2952.

Steinberg, C., Eisenächer, K., Gross, O., Reindl, W., Schmitz, F., Ruland, J., and Krug, A. (2009). The IFN regulatory factor 7-dependent type I IFN response is not essential for early resistance against murine cytomegalovirus infection. Eur. J. Immunol. *39*, 1007–1018.

Swiecki, M., Gilfillan, S., Vermi, W., Wang, Y., and Colonna, M. (2010). Plasmacytoid dendritic cell ablation impacts early interferon responses and antiviral NK and CD8(+) T cell accrual. Immunity *33*, 955–966.

Tabeta, K., Georgel, P., Janssen, E., Du, X., Hoebe, K., Crozat, K., Mudd, S., Shamel, L., Sovath, S., Goode, J., et al. (2004). Toll-like receptors 9 and 3 as essential components of innate immune defense against mouse cytomegalovirus infection. Proc. Natl. Acad. Sci. USA *101*, 3516–3521.

Tischer, B.K., Smith, G.A., and Osterrieder, N. (2010). En passant mutagenesis: a two step markerless red recombination system. Methods Mol. Biol. *634*, 421–430.

Zucchini, N., Bessou, G., Robbins, S.H., Chasson, L., Raper, A., Crocker, P.R., and Dalod, M. (2008a). Individual plasmacytoid dendritic cells are major contributors to the production of multiple innate cytokines in an organ-specific manner during viral infection. Int. Immunol. *20*, 45–56.

Zucchini, N., Bessou, G., Traub, S., Robbins, S.H., Uematsu, S., Akira, S., Alexopoulou, L., and Dalod, M. (2008b). Cutting edge: overlapping functions of TLR7 and TLR9 for innate defense against a herpesvirus infection. J. Immunol. *180*, 5799–5803.